



Estimating effective contact and flight times using a sacral-mounted inertial measurement unit

Aurélien Patoz^{a,b,*}, Thibault Lussiana^{b,c,d}, Bastiaan Breine^{b,e}, Cyrille Gindre^{b,c}, Davide Malatesta^a

^a Institute of Sport Sciences, University of Lausanne, Lausanne 1015, Switzerland

^b Research and Development Department, Volodalen Swiss Sport Lab, Aigle 1860, Switzerland

^c Research and Development Department, Volodalen, Chavéria 39270, France

^d Research Unit EA3920 Prognostic Markers and Regulatory Factors of Cardiovascular Diseases and Exercise Performance, Health, Innovation platform, University of Franche-Comté, Besançon, France

^e Department of Movement and Sports Sciences, Ghent University, Ghent 9000, Belgium

ARTICLE INFO

Keywords:

Gait analysis
Running
Biomechanics
Sensor
Accelerometer

ABSTRACT

Effective ground contact (t_{ce}) and flight (t_{fe}) times were proven to be more appropriate to decipher the landing-take-off asymmetry of running than usual ground contact (t_c) and flight (t_f) times. To measure these effective timings, force plate is the gold standard method (GSM), though not very portable overground. In such situation, alternatives could be to use portable tools such as inertial measurement unit (IMU). Therefore, the purpose of this study was to propose a method that uses the vertical acceleration recorded using a sacral-mounted IMU to estimate t_{ce} and t_{fe} and to compare these estimations to those from GSM. Besides, t_{ce} and t_{fe} were used to evaluate the landing-take-off asymmetry, which was further compared to GSM. One hundred runners ran at 9, 11, and 13 km/h. Force data (200 Hz) and IMU data (208 Hz) were acquired by an instrumented treadmill and a sacral-mounted IMU, respectively. The comparison between GSM and IMU method depicted root mean square error ≤ 22 ms ($\leq 14\%$) for t_{ce} and t_{fe} along with small systematic biases (≤ 20 ms) for each tested speed. These errors are similar to previously published methods that estimated usual t_c and t_f . The systematic biases on t_{ce} and t_{fe} were subtracted before calculating the landing-take-off asymmetry, which permitted to correctly evaluate it at a group level. Therefore, the findings of this study support the use of this method based on vertical acceleration recorded using a sacral-mounted IMU to estimate t_{ce} and t_{fe} for level treadmill runs and to evaluate the landing-take-off asymmetry but only after subtraction of systematic biases and at a group level.

1. Introduction

Back in 1988, Cavagna et al. (1988) defined two key running parameters denoted as effective ground contact (t_{ce}) and flight (t_{fe}) times. They differ from the usual ground contact (t_c) and flight (t_f) times by the fact that t_{ce} and t_{fe} correspond to the amount of time where the vertical ground reaction force is above and below body weight, respectively, rather than where the foot is in contact with the ground or not (Cavagna et al., 2008a). These effective timings were proven to be more appropriate to decipher the landing-take-off asymmetry of running than the usual timings (i.e., t_c and t_f) (Cavagna, 2006; Cavagna et al., 2008a, b).

These two parameters are usually obtained from effective foot-strike (eFS) and toe-off (eTO) events, i.e., when vertical ground reaction force

goes over and below body weight, respectively. To obtain such events, the use of force plates is considered as the gold standard method (GSM). However, force plates are not always available and not very portable overground (Abendroth-Smith, 1996; Maiwald et al., 2009). To overcome such limitation, gait events detection methods were developed using inertial measurement units (IMU) (Chew et al., 2018; Day et al., 2021; Falbriard et al., 2018, 2020; Flaction et al., 2013; Giandolini et al., 2016; Giandolini et al., 2014; Gindre et al., 2016; Lee et al., 2010; Moenilssen, 1998; Norris et al., 2014). Amongst them, a natural choice is a sacral-mounted IMU, the reason being that such placement approximates the location of the center of mass (Napier et al., 2020).

On the one hand, Flaction et al. (2013) determined effective timings using the Myotest® but did not explicitly mentioned the exact procedure

* Corresponding author.

E-mail address: aurelien.patoz@unil.ch (A. Patoz).

<https://doi.org/10.1016/j.jbiomech.2021.110667>

Accepted 28 July 2021

Available online 31 July 2021

0021-9290/© 2021 The Authors. Published by Elsevier Ltd. This is an open access article under the CC BY license (<http://creativecommons.org/licenses/by/4.0/>).

to go from raw IMU data to effective timings. Moreover, the Myotest® outcomes were compared to t_c and t_f from photocell- and optical-based systems instead of t_{ce} and t_{fe} from GSM, leading to an “unusable” validity assessment (Gindre et al., 2016). On the other hand, Day et al. (2021) calculated t_c and t_f from usual foot-strike and toe-off events obtained using a 0 N threshold applied to an estimation of the vertical ground reaction force (using Newton’s second law of motion). However, the authors did not attempt to calculate t_{ce} and t_{fe} . Nonetheless, they showed that a 5 Hz low-pass filter was resulting in the best correlation between t_c obtained from GSM and their method, though mentioning that more research investigating the effect of different filtering methods is needed. For this reason, the purpose of this study was to estimate t_{ce} and t_{fe} using a different filtering method than the one proposed by Day et al. (2021), i. e., a Fourier series truncated to 5 Hz instead of a 5 Hz low-pass filter, to filter the sacral-mounted IMU data (IMU method; IMUM) and to compare these estimations to those from GSM. Besides, estimated t_{ce} and t_{fe} were used to evaluate the landing-take-off asymmetry of running and compare it to that obtained using GSM.

2. Materials and methods

2.1. Participant characteristics

Hundred recreational runners, 74 males (age: 30 ± 8 years, height: 180 ± 6 cm, body mass: 71 ± 7 kg, and weekly running distance: 37 ± 22 km) and 26 females (age: 30 ± 7 years, height: 169 ± 5 cm, body mass: 61 ± 6 kg, and weekly running distance: 22 ± 16 km) voluntarily participated in this study. For study inclusion, participants were required to do not have current or recent lower-extremity injury (≤ 1 month). The study protocol was approved by the local Ethics Committee (CER-VD 2020-00334) and each participant gave written informed consent.

2.2. Experimental procedure and data collection

After providing written informed consent, an IMU of 9.4 g (Movesense, Vantaa, Finland) was firmly attached to the sacrum at the midpoint between the posterior superior iliac spinae (Fig. 1) using an elastic strap belt (Movesense, Vantaa, Finland). Then, a 7-min warm-up run (9–13 km/h) was performed on an instrumented treadmill (Arsalis T150-FMT-MED, Louvain-la-Neuve, Belgium), followed by three 1-min runs (9, 11, and 13 km/h) performed in a randomized order. Three-dimensional (3D) kinetic and IMU data were collected during the first 10 strides following the 30-s mark of running trials.



Fig. 1. The Movesense inertial measurement unit attached to the sacrum of a representative participant using an elastic strap belt.

3D kinetic data were collected at 200 Hz using the force plate embedded into the treadmill and Vicon Nexus software v2.9.3 (Vicon, Oxford, United-Kingdom), and processed in Visual3D Professional software v6.01.12 (C-Motion, Germantown, USA). Ground reaction forces were interpolated using a third-order polynomial least-square fit algorithm and low-pass filtered at 20 Hz using a fourth-order Butterworth filter (Swinnen et al., 2021).

IMU data were collected at 208 Hz (manufacturing specification) with a saturation range of ± 8 g, and using an iPhone SE (Apple, Cupertino, USA) and a home-made iOS application that communicated with the IMU via Bluetooth. During each running trial, the iPhone was kept close to the participant (≤ 1 m) to avoid losing the Bluetooth connection. Kinetic and IMU data were not exactly synchronized (Fig. 2).

2.3. Gold standard method

eFS and eTO were identified within Visual3D by applying a body weight threshold to the vertical ground reaction force (Cavagna et al., 1988). Then, t_{ce} was given by the time between eFS and eTO while t_{fe} by

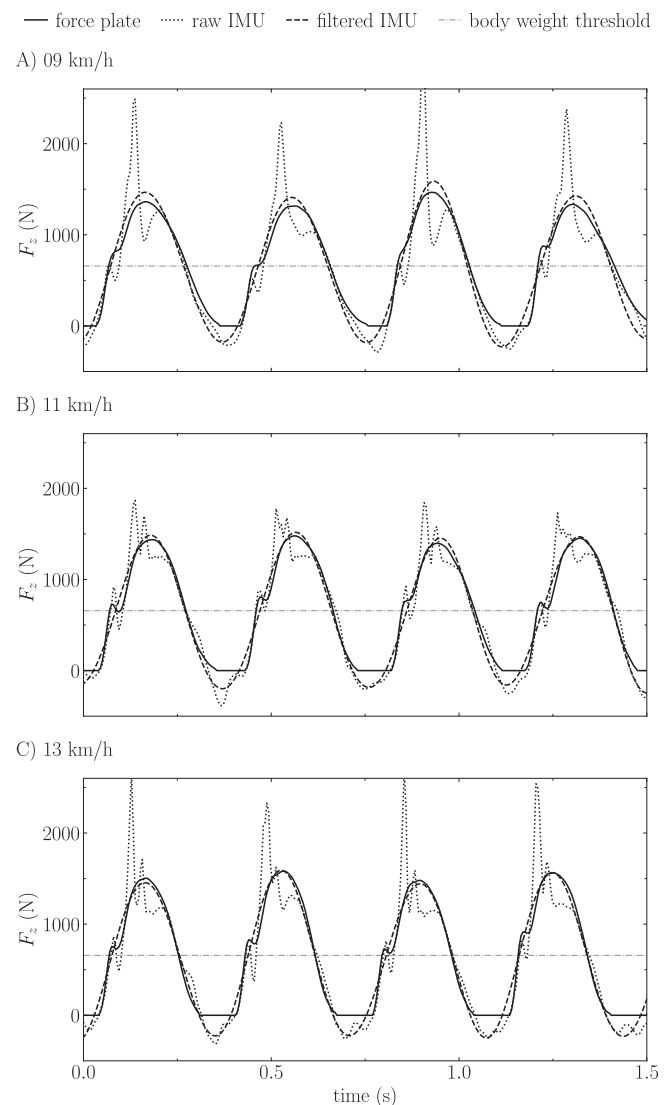


Fig. 2. Vertical ground reaction force (F_z) obtained using force plate (gold standard; solid line) and inertial measurement unit (IMU; raw: dotted line and filtered: dashed line) during two running strides for a given participant at A) 9 km/h, B) 11 km/h, and C) 13 km/h. The gray dash-dotted line represents the body weight threshold used to detect effective foot-strike and toe-off events.

the time between eTO and eFS.

2.4. Inertial measurement unit method

A custom c++ code (ISO/IEC, 2020) was used to process IMU data. First, the z-axis of IMU was aligned with z-axis of local coordinate system (Appendix A). Then, aligned raw acceleration data were filtered using a truncated Fourier series to 5 Hz. This cut-off frequency was chosen because it led to the best estimation of t_c in Day et al. (2021). Filtered data were used to detect eFS and eTO using a $g = 9.81 \text{ m/s}^2$ threshold (equivalent to the body weight threshold of GSM), and to reconstruct vertical ground reaction force by multiplying it by body mass. Besides, t_{ce} and t_{fe} were calculated from eFS and eTO (Appendix B).

2.5. Data analysis

Root mean square error [RMSE; in absolute (ms) and relative units, i. e., normalized by the corresponding mean value over all participants and obtained using GSM] was calculated for t_{ce} and t_{fe} . RMSE was computed from t_{ce} and t_{fe} averaged over the 10 analyzed strides for each participant and each running trial. Data analysis was performed using Python (v3.7.4, available at <http://www.python.org>).

2.6. Statistical analysis

All data are presented as mean \pm standard deviation. Systematic bias, lower and upper limit of agreements, and 95% confidence intervals between GSM and IMUM for t_{ce} and t_{fe} were examined using Bland-Altman plots for each speed (Atkinson and Nevill, 1998; Bland and Altman, 1995). Systematic biases have a direction, i.e., positive values indicate overestimations of IMUM while negative values indicate

underestimations. Proportional bias was identified by a significant slope of the regression line. Coefficients of determination (R^2) were computed to assess the quality of the linear fit. t_{ce} and t_{fe} obtained using IMUM and GSM were compared using two-way [method of calculation (GSM vs. IMUM) \times running speed (9 vs. 11 vs. 13)] repeated measures ANOVA with Mauchly's correction for sphericity and employing Holm corrections for pairwise post hoc comparisons. Differences between GSM and IMUM were quantified using Cohen's d effect size and interpreted as very small, small, moderate, and large when $|d|$ values were close to 0.01, 0.2, 0.5, and 0.8, respectively (Cohen, 1988). The landing-take-off asymmetry was evaluated as the difference between t_{fe} and t_{ce} (Δ) (Cavagna, 2006; Cavagna et al., 2008a, b). Δ obtained using IMUM and GSM were compared using two-way repeated measures ANOVA and differences between GSM and IMUM were also quantified using Cohen's d effect size. Statistical analysis was performed using Jamovi (v1.2, retrieved from <https://www.jamovi.org>) with a level of significance set at $P \leq 0.05$.

3. Results

Fig. 2 depicts the vertical ground reaction force obtained using GSM (force plate) and IMUM (raw and filtered IMU).

t_{ce} and t_{fe} depicted small systematic biases (≤ 20 ms) at all speeds. The smallest absolute bias was given for 9 km/h, followed by 11 km/h and 13 km/h (Fig. 3 and Table 1). Both effective timings reported a significant negative proportional bias at all speeds but were accompanied with small R^2 (Table 1).

Significant effects for both method of calculation and running speed as well as an interaction effect were depicted by repeated measures ANOVA for t_{ce} and t_{fe} ($P < 0.001$; Table 2). Significant differences between GSM and IMUM for t_{ce} and t_{fe} at all speeds ($P < 0.001$) were

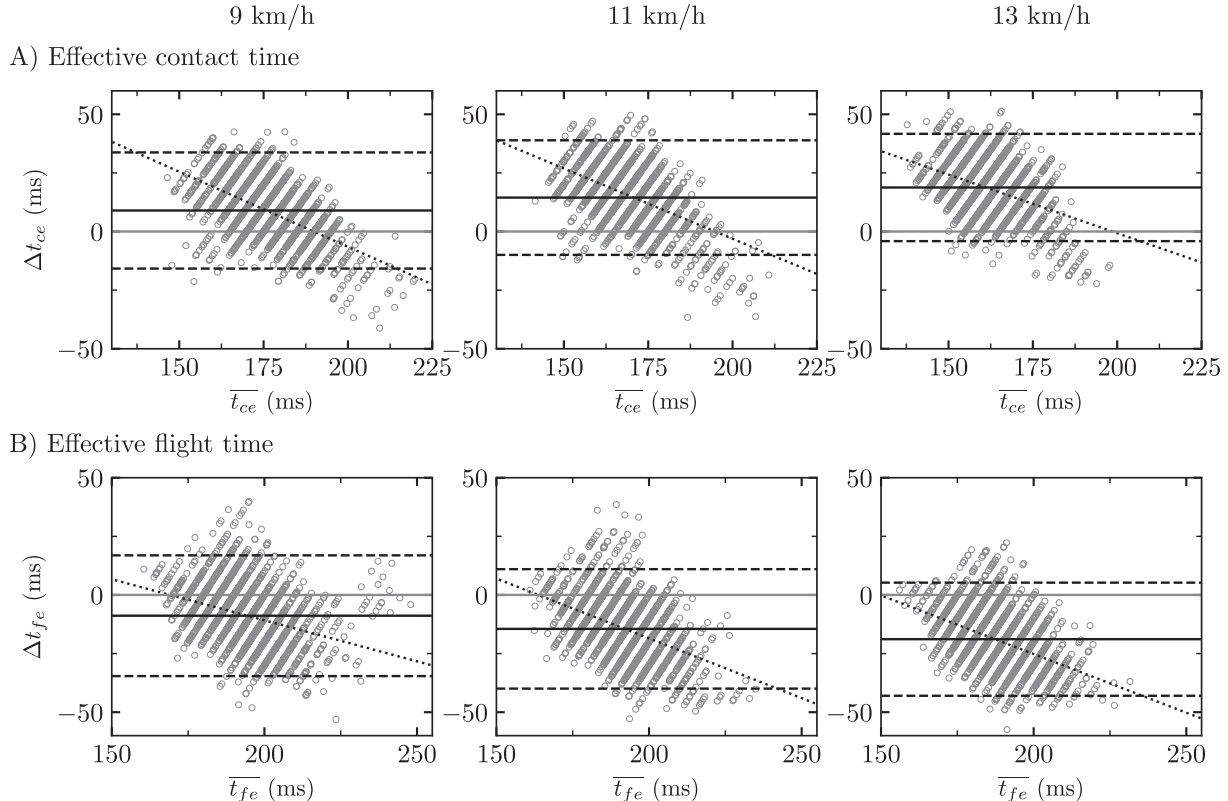


Fig. 3. Comparison of A) effective contact time (t_{ce}) and B) effective flight time (t_{fe}) obtained using inertial measurement unit method and gold standard method [differences (Δ) as function of mean values together with systematic bias (black solid line) as well as lower and upper limit of agreements (black dashed lines), and proportional bias (black dotted line), i.e., Bland-Altman plots] for three running speeds. For systematic bias, positive and negative values indicate the inertial measurement unit method overestimated and underestimated t_{ce} and t_{fe} , respectively.

Table 1

Systematic bias, lower limit of agreement (lloa), upper limit of agreement (uloa), proportional bias \pm residual random error together with its corresponding *P*-value, and coefficient of determination (R^2) between effective contact (t_{ce}) and flight (t_{fe}) times obtained using inertial measurement unit method and gold standard method at three running speeds. 95% confidence intervals are given in square brackets [lower, upper]. Significant ($P \leq 0.05$) proportional bias are reported in bold font. For systematic bias, positive and negative values indicate the inertial measurement unit method overestimated and underestimated t_{ce} and t_{fe} , respectively.

	Running Speed (km/h)	Systematic Bias	lloa	uloa	Proportional Bias (<i>P</i>)	R^2
t_{ce} (ms)	9	9.0 [8.4, 9.5]	-15.8 [-16.7, -14.9]	33.7 [32.8, 34.7]	-0.64 \pm 0.02 (<0.001)	0.30
	11	14.5 [13.9, 15.0]	-10.0 [-10.9, -9.0]	38.9 [38.0, 39.8]	-0.60 \pm 0.02 (<0.001)	0.25
	13	18.8 [18.3, 19.3]	-4.1 [-5.0, -3.2]	41.7 [40.8, 42.5]	-0.50 \pm 0.03 (<0.001)	0.15
t_{fe} (ms)	9	-8.9 [-9.4, -8.3]	-34.6 [-35.6, -33.6]	16.9 [15.9, 17.9]	-0.35 \pm 0.02 (<0.001)	0.10
	11	-14.5 [-15.0, -13.9]	-39.9 [-40.9, -39.0]	11.0 [10.0, 12.0]	-0.51 \pm 0.02 (<0.001)	0.18
	13	-18.9 [-19.4, -18.3]	-43.0 [-43.9, -42.1]	5.3 [4.3, 6.2]	-0.50 \pm 0.02 (<0.001)	0.19

Table 2

Effective contact (t_{ce}) and flight (t_{fe}) times obtained using gold standard method (GSM) and inertial measurement unit method (IMUM) together with root mean square error [RMSE; both in absolute (ms or N) and relative (%) units], as well as Cohen's *d* effect size for three running speeds. Significant ($P \leq 0.05$) method of calculation, running speed, and interaction effect, as determined by repeated measures ANOVA, are reported in bold font. *Significant difference between t_{ce} and t_{fe} obtained using GSM and IMUM, as determined by Holm post hoc tests.

Running Speed (km/h)		t_{ce} (ms)	t_{fe} (ms)
9	GSM	172.2 \pm 14.4*	198.6 \pm 14.3*
	IMUM	181.2 \pm 8.0	189.8 \pm 10.3
	RMSE (ms)	14.7	14.8
	RMSE (%)	8.5	7.4
	<i>d</i>	-0.71	0.65
11	GSM	162.5 \pm 13.6*	198.7 \pm 13.8*
	IMUM	177.0 \pm 8.1	184.2 \pm 8.4
	RMSE (ms)	18.5	18.6
	RMSE (%)	11.4	9.4
	<i>d</i>	-1.21	1.14
13	GSM	152.7 \pm 12.0*	197.3 \pm 13.3*
	IMUM	171.5 \pm 7.9	178.4 \pm 8.0
	RMSE (ms)	21.6	21.7
	RMSE (%)	14.2	11.0
	<i>d</i>	-1.72	1.51
Method of calculation effect		$P < 0.001$	$P < 0.001$
Running speed effect		$P < 0.001$	$P < 0.001$
Interaction effect		$P < 0.001$	$P < 0.001$

Values are presented as mean \pm standard deviation.

reported by Holm post hoc tests. RMSE was ≤ 22 ms ($\leq 14\%$) for t_{ce} and t_{fe} (Table 2) and Cohen's *d* effect size was large for t_{ce} and t_{fe} except at 9 km/h which was moderate (Table 2).

Due to the presence of systematic biases for t_{ce} and t_{fe} obtained by IMUM (Table 1), Δ was also estimated from these t_{ce} and t_{fe} but with further subtracting the systematic biases (corrected IMUM). Significant effects for both method of calculation and running speed as well as an interaction effect were depicted by repeated measures ANOVA for Δ ($P < 0.001$; Table 3). Holm post hoc tests reported significantly larger Δ for GSM than IMUM and for corrected IMUM than IMUM at all speeds ($P < 0.001$) whereas GSM and corrected IMUM were not statistically different ($P = 1.0$). Cohen's *d* effect size was large between GSM and IMUM but very small between GSM and corrected IMUM at all speeds (Table 3). Noteworthy, proportional biases were not taken into account because their corresponding R^2 (≤ 0.30) were not satisfactory. Indeed, using proportional biases to correct t_{ce} and t_{fe} resulted in a worse estimation of Δ than with corrected IMUM (data not shown).

4. Discussion

Our findings demonstrated systematic and proportional biases between GSM and IMUM for t_{ce} and t_{fe} at each speed employed as well as significant differences between GSM and IMUM. Nonetheless, systematic biases were small (≤ 20 ms). In addition, after subtraction of these systematic biases, the landing-take-off asymmetry was correctly

Table 3

Landing-take-off asymmetry (Δ), i.e., the difference between effective flight and effective contact times, obtained using gold standard method (GSM), inertial measurement unit method (IMUM), and corrected IMUM (subtraction of systematic biases on effective flight and effective contact times), as well as Cohen's *d* effect size between GSM and IMUM and between GSM and corrected IMUM for three running speeds. Significant ($P \leq 0.05$) method of calculation, running speed, and interaction effect, as determined by repeated measures ANOVA, are reported in bold font. * and † denote a significant difference between Δ obtained using GSM and IMUM and using IMUM and corrected IMUM, respectively, as determined by Holm post hoc tests.

Running Speed (km/h)		Δ (ms)
9	GSM	26.4 \pm 23.0*
	IMUM	8.6 \pm 7.0
	corrected IMUM	26.5 \pm 7.0 [†]
	<i>d</i> (IMUM)	0.96
	<i>d</i> (corrected IMUM)	0.00
11	GSM	36.2 \pm 22.1*
	IMUM	7.2 \pm 3.7
	corrected IMUM	36.2 \pm 3.7 [†]
	<i>d</i> (IMUM)	1.67
	<i>d</i> (corrected IMUM)	0.00
13	GSM	44.6 \pm 20.1*
	IMUM	6.9 \pm 2.4
	corrected IMUM	44.6 \pm 3.4 [†]
	<i>d</i> (IMUM)	-2.32
	<i>d</i> (corrected IMUM)	0.0
Method of calculation effect		$P < 0.001$
Running speed effect		$P < 0.001$
Interaction effect		$P < 0.001$

Values are presented as mean \pm standard deviation.

evaluated by corrected IMUM at a group level. However, as revealed by the small standard deviations obtained for corrected IMUM, the landing-take-off asymmetry was not as correctly evaluated at an individual than at a group level.

IMUM reported systematic biases ≤ 20 ms and RMSE ≤ 22 ms ($\leq 14\%$) for t_{ce} (Tables 1 and 2). Noteworthy, error in t_{fe} (in absolute units) tends to be equal to the one in t_{ce} when the number of strides per individual tends to infinity. Indeed, the only difference to calculate t_{ce} and t_{fe} being in the first eFS and last eTO. In addition, errors in t_{ce} and t_{fe} could not directly be compared to the actual literature because, to the best of our knowledge, no study comparing several methods to calculate these effective timings was conducted so far. Indeed, we are only aware of the comparison between t_{ce} and t_{fe} obtained using Myotest® and t_c and t_f obtained from photocell- and optical-based systems (Gindre et al., 2016), which makes this comparison useless as different outcomes (t_{ce} vs. t_c and t_{fe} vs. t_f) were actually being compared. Nevertheless, the authors were aware of this limitation and clearly stated this limitation (Gindre et al., 2016).

Errors in t_{ce} and t_{fe} could be compared to those obtained for usual timings (t_c and t_f). For instance, the errors reported in this study seemed to be smaller than the one obtained for t_c by Day et al. (2021) though bias and RMSE were not explicitly given [~ 30 ms by visual inspection

of their Fig. 5 (14–19 km/h)]. As for foot-worn inertial sensors, a systematic bias on t_c of ~ 10 ms (10–20 km/h) (Falbriard et al., 2018) and RMSE of ~ 10 ms (11 km/h) (Chew et al., 2018) were reported, which placed IMUM at a similar level of accuracy. In addition, Falbriard et al. (2018) depicted a proportional bias for t_c , as in this study for t_{ce} . Besides, IMUM showed similar accuracy than an opoelectronic system (3D kinematic data), which reported RMSE ≥ 15 ms for t_c (20 km/h) (Smith et al., 2015). However, such system suffers from a lack of portability and do not allow continuous data collection. For this reason, using a single IMU was advantageous by its portability, and was shown to be quite accurate to estimate t_{ce} (and t_{fe}). Moreover, in practice, a systematic subtraction of the bias corresponding to the given speed could be applied when estimating t_{ce} and t_{fe} .

Due to the inexact synchronization between kinetic and IMU data, eFS and eTO could not be compared between GSM and IMUM. However, we suspect that even under perfect synchronization, eFS and eTO from GSM and IMUM would not exactly coincide as vertical force used in IMUM is an approximation of ground truth vertical force recorded by force plate. Nonetheless, further studies involving synchronized kinetic and IMU data would prove useful, especially if one is interested in assessing metrics at specific eFS and eTO, for instance using additional IMUs (Favre et al., 2008) themselves synchronized with the sacral-mounted one which would provide eFS and eTO.

A single cut-off frequency was used to filter the vertical ground reaction force, i.e., 20 Hz. Though this choice of cut-off frequency is quite widespread (Mai and Willwacher, 2019; Swinnen et al., 2021), other cut-off frequencies (e.g., 30 or 80 Hz) are also used in the literature (Alcantara et al., 2021; Breine et al., 2017). In this case, the error of IMUM might increase because the cut-off frequency affects the magnitude of the vertical ground reaction force and thus the time at which eFS and eTO occur. Hence, it would also be useful to explore the effect of the cut-off frequency of the truncated Fourier series on the accuracy of IMUM, as already explored by Day et al. (2021) for a low-pass filter. Additionally, the effect of the filter itself (e.g., truncated Fourier series, 4th order low-pass Butterworth filter, 8th order low-pass Butterworth filter, etc.) might also be worth exploring. Therefore, further studies investigating the effect of the cut-off frequency of both the gold standard and IMU signals as well as the kind of filter should be conducted. Furthermore, a significant effect of running speed was observed for t_{ce} and t_{fe} (Table 2). The most accurate estimation (smallest systematic bias and RMSE) was given at 9 km/h (Fig. 3 and Tables 1 and 2). These findings suggests that the cut-off frequency that estimates best t_{ce} and t_{fe} might be speed dependent and reinforce the need to further explore the effect of the cut-off frequency of both GSM and IMUM, and to explore slower and faster speeds.

The landing-take-off asymmetry was reported to increase from ~ 20 to ~ 50 ms with increasing running speed (8–20 km/h) (Cavagna, 2006; Cavagna et al., 2008a, b). The present study depicted that Δ increased from 25 to 45 ms with running speed (9–13 km/h) for GSM and for corrected IMUM while Δ was ~ 7 ms at all tested speeds for IMUM. Due to the systematic biases reported for t_{fe} and t_{ce} , though similar than previously published methods that estimated usual t_f and t_c , IMUM was not able to evaluate the landing-take-off asymmetry. The main reason was that t_{fe} and t_{ce} were underestimated and overestimated, respectively, leading to an accumulation of errors. Moreover, the deviation from GSM increased with increasing speed because the error on t_{fe} and t_{ce} also increased with speed. However, after subtraction of these systematic biases, the landing-take-off asymmetry was correctly evaluated by corrected IMUM at a group level. Nonetheless, even though these biases might be generalizable due to the large dataset employed, i.e., 100 runners, they might still be dependent on the given dataset. Therefore, we suggest researchers willing to employ this method to first calculate these biases using their own dataset and then subtract these calculated biases to evaluate the landing-take-off asymmetry. Finally, the landing-

take-off-asymmetry evaluated by corrected IMUM reported small standard deviations (Table 3), meaning that the landing-take-off asymmetry was not as correctly evaluated at an individual than at a group level. Indeed, corrected IMUM was not totally able to provide insights into the inter-individual variation of the landing-take-off asymmetry.

This study presents few limitations. The comparison between IMUM and GSM was performed using treadmill runs. As spatiotemporal parameters between overground and treadmill running are largely comparable, IMUM might also perform well overground (Van Hooren et al., 2020). However, it was concluded that participants behaved differently when attempting to achieve faster speeds overground than on a treadmill (Bailey et al., 2017). Therefore, the comparison between IMUM and GSM using additional conditions (i.e., faster speeds, positive and negative slopes, and different types of ground) should be further studied.

5. Conclusion

A IMUM was provided to estimate t_{ce} and t_{fe} . These timings were obtained by filtering the vertical acceleration recorded by a sacral-mounted IMU using a truncated Fourier series to 5 Hz. GSM and IMUM depicted RMSE ≤ 22 ms ($\leq 14\%$) together with small systematic biases (≤ 20 ms) for t_{ce} and t_{fe} at each speed. These errors are similar to previously published methods that estimated usual t_c and t_f . To avoid that the errors on t_{ce} and t_{fe} accumulate when evaluating the landing-take-off asymmetry, the systematic biases on t_{ce} and t_{fe} were subtracted before calculating the landing-take-off asymmetry, which permitted to correctly evaluate it at a group level. Therefore, the findings of this study support the use of this method based on vertical acceleration recorded using a sacral-mounted IMU to estimate t_{ce} and t_{fe} for level treadmill runs and to evaluate the landing-take-off asymmetry of running but only after subtraction of systematic biases and at a group level.

CRedit authorship contribution statement

Aurélien Patoz: Conceptualization, Methodology, Investigation, Formal analysis, Writing – original draft, Writing – review & editing, Supervision. **Thibault Lussiana:** Conceptualization, Methodology, Investigation, Writing – review & editing, Supervision. **Bastiaan Breine:** Investigation, Formal analysis, Writing – original draft, Writing – review & editing. **Cyrille Gindre:** Conceptualization, Methodology, Writing – review & editing, Supervision. **Davide Malatesta:** Conceptualization, Methodology, Writing – review & editing, Supervision.

Declaration of Competing Interest

The authors declare that they have no known competing financial interests or personal relationships that could have appeared to influence the work reported in this paper.

Acknowledgements

The authors warmly thank the participants for their time and cooperation.

Funding

This study was supported by the Innosuisse grant no. 35793.1 IP-LS.

Availability of Data and Material

The datasets supporting this article are available on request to the corresponding author.

Appendix A. . Aligning the IMU z-axis with the z-axis of the local coordinate system

The laboratory coordinate system (LCS) was oriented such that x -, y -, and z -axis denoted medio-lateral (pointing towards the right side of the body), posterior-anterior, and inferior-superior axis, respectively. The IMU was oriented such that its own x -, y -, and z -axes denoted medio-lateral (pointing towards the right side of the IMU), posterior-anterior, and inferior-superior axis, respectively.

Raw acceleration data was filtered using a truncated Fourier series to 0.5 Hz in each dimension, allowing to remove any acceleration due to movement of the IMU (vibrations and body motion) (Day et al., 2021). Indeed, a truncated Fourier series allows removing any frequency component within the original signal that are above the requested cut-off. Noteworthy, the number of terms to include in the truncated Fourier series is given by $N = nF/f$, where n is the number of IMU data points, F is the requested truncation frequency, and f is the IMU sampling frequency. Then, the median of each component of the filtered 3D signal was computed. Knowing that the average acceleration should be equal to g in the z -axis of LCS and 0 in the other two axes, the average angle between the z -axis of IMU and LCS could be calculated based on the previously computed medians. This average angle corresponds to the average tilt of the IMU with respect to the z -axis of LCS. Therefore, the IMU can be reoriented using this average angle so that its z -axis is, in average, aligned with the one of LCS. However, it was assumed that the rotational motion of the sensor around any of the three axes was negligible so that no complicated reorientation of the IMU had to be performed at each timestamp, which would anyway require several approximations (see for instance Falbriard et al. (2020) for foot-worn IMU). This reorientation process is usually not taken into account when using sacral-mounted IMU and signals from sacral-mounted IMU are usually analyzed along the IMU's coordinate system and compared to ground reaction forces analyzed in LCS (Alcantara et al., 2021; Day et al., 2021; Lee et al., 2010).

Appendix B. . Computing t_{ce} and t_{fe} from eFS and eTO obtained using the sacral-mounted IMU

t_{ce} was given by the time between eFS and eTO data points while t_{fe} by the time between eTO data point $+1$ and eFS data point -1 . Doing so, two timesteps were missing when computing t_{ce} and t_{fe} for a running step. However, this was corrected by using a linear interpolation to calculate the “exact” timing of the threshold for eFS and eTO, using eFS data point and previous data point and eTO data point and next data point, respectively. Then, the duration between exact eFS threshold and eFS data point as well as between eTO data point and exact eTO threshold were added to t_{ce} while the duration between eFS data point -1 and exact eFS threshold as well as between exact eTO threshold and eTO data point $+1$ were added to t_{fe} . This procedure allowed to obtain the exact (under linear interpolation) t_{ce} and t_{fe} falling above and below the threshold, respectively.

References

- Abendroth-Smith, J., 1996. Stride adjustments during a running approach toward a force plate. *Res. Q. Exerc. Sport* 67 (1), 97–101.
- Alcantara, R.S., Day, E.M., Hahn, M.E., Grabowski, A.M., 2021. Sacral acceleration can predict whole-body kinetics and stride kinematics across running speeds. *e11199 PeerJ* 9.
- Atkinson, G., Nevill, A.M., 1998. Statistical methods for assessing measurement error (reliability) in variables relevant to sports medicine. *Sports Med.* 26 (4), 217–238.
- Bailey, J.P., Mata, T., Mercer, J.D., 2017. Is the relationship between stride length, frequency, and velocity influenced by running on a treadmill or overground? *International Journal of Exercise Science* 10, 1067–1075.
- Bland, J.M., Altman, D.G., 1995. Comparing methods of measurement: why plotting difference against standard method is misleading. *Lancet* 346 (8982), 1085–1087.
- Breine, B., Malcolm, P., Van Caekenbergh, I., Fiers, P., Frederick, E.C., De Clercq, D., 2017. Initial foot contact and related kinematics affect impact loading rate in running. *J. Sports Sci.* 35 (15), 1556–1564.
- Cavagna, G.A., 2006. The landing–take-off asymmetry in human running. *J. Exp. Biol* 209 (20), 4051–4060.
- Cavagna, G.A., Franzetti, P., Heglund, N.C., Willems, P., 1988. The determinants of the step frequency in running, trotting and hopping in man and other vertebrates. *The Journal of Physiology* 399, 81–92.
- Cavagna, G.A., Legramandi, M.A., Peyré-Tartaruga, L.A., 2008a. The landing–take-off asymmetry of human running is enhanced in old age. *J. Exp. Biol* 211 (10), 1571–1578.
- Cavagna, G.A., Legramandi, M.A., Peyré-Tartaruga, L.A., 2008b. Old men running: mechanical work and elastic bounce. *Proc. Biol. Sci.* 275 (1633), 411–418.
- Chew, D.-K., Ngoh, K.-H., Gouwanda, D., Gopalai, A.A., 2018. Estimating running spatial and temporal parameters using an inertial sensor. *Sports Eng.* 21 (2), 115–122.
- Cohen, J., 1988. *Statistical Power Analysis for the Behavioral Sciences*. Routledge.
- Day, E.M., Alcantara, R.S., McGeehan, M.A., Grabowski, A.M., Hahn, M.E., 2021. Low-pass filter cutoff frequency affects sacral-mounted inertial measurement unit estimations of peak vertical ground reaction force and contact time during treadmill running. *J. Biomech.* 119, 110323.
- Falbriard, M., Meyer, F., Mariani, B., Millet, G.P., Aminian, K., 2018. Accurate Estimation of Running Temporal Parameters Using Foot-Worn Inertial Sensors. *Front Physiol* 9.
- Falbriard, M., Meyer, F., Mariani, B., Millet, G.P., Aminian, K., 2020. Drift-Free Foot Orientation Estimation in Running Using Wearable IMU. *Frontiers in Bioengineering and Biotechnology* 8.
- Favre, J., Jolles, B.M., Aissaoui, R., Aminian, K., 2008. Ambulatory measurement of 3D knee joint angle. *J. Biomech.* 41 (5), 1029–1035.
- Flaction, P., Quievre, J., Morin, J.B., 2013. *An Athletic Performance Monitoring Device*, Washington, DC: U.S. Patent and Trademark Office.
- Giandolini, M., Horvais, N., Rossi, J., Millet, G.Y., Samozino, P., Morin, J.-B., 2016. Foot strike pattern differently affects the axial and transverse components of shock acceleration and attenuation in downhill trail running. *J. Biomech.* 49 (9), 1765–1771.
- Giandolini, M., Poupard, T., Gimenez, P., Horvais, N., Millet, G.Y., Morin, J.-B., Samozino, P., 2014. A simple field method to identify foot strike pattern during running. *J. Biomech.* 47 (7), 1588–1593.
- Gindre, C., Lussiana, T., Hebert-Losier, K., Morin, J.-B., 2016. Reliability and validity of the Myotest® for measuring running stride kinematics. *J. Sports Sci.* 34 (7), 664–670.
- ISO, IEC, 2020. *ISO International Standard ISO/IEC 14882:2020(E) Programming languages — C++*. International Organization for Standardization, Geneva, Switzerland.
- Lee, James B., Mellifont, Rebecca B., Burkett, Brendan J., 2010. The use of a single inertial sensor to identify stride, step, and stance durations of running gait. *J. Sci. Med. Sport* 13 (2), 270–273.
- Mai, Patrick, Willwacher, Steffen, 2019. Effects of low-pass filter combinations on lower extremity joint moments in distance running. *J. Biomech.* 95, 109311.
- Maiwald, C., Sterzing, T., Mayer, T.A., Milani, T.L., 2009. Detecting foot-to-ground contact from kinematic data in running. *Footwear Science* 1 (2), 111–118.
- Moe-Nilssen, R., 1998. A new method for evaluating motor control in gait under real-life environmental conditions. Part 1: The instrument. *Clin. Biomech.* 13 (4-5), 320–327.
- Napier, Christopher, Jiang, Xianta, MacLean, Christopher L., Menon, Carlo, Hunt, Michael A., 2020. The use of a single sacral marker method to approximate the centre of mass trajectory during treadmill running. *J. Biomech.* 108, 109886.
- Norris, Michelle, Anderson, Ross, Kenny, Ian C., 2014. Method analysis of accelerometers and gyroscopes in running gait: A systematic review. *Proceedings of the Institution of Mechanical Engineers, Part P. Journal of Sports Engineering and Technology* 228 (1), 3–15.
- Smith, Laura, Preece, Stephen, Mason, Duncan, Bramah, Christopher, 2015. A comparison of kinematic algorithms to estimate gait events during overground running. *Gait Posture* 41 (1), 39–43.
- Swinnen, W., Mylle, I., Hoogkamer, W., De Groot, F., Vanwansseele, B., 2021. Changing Stride Frequency Alters Average Joint Power and Power Distributions during Ground Contact and Leg Swing in Running. *Med. Sci. Sports Exerc.*
- Van Hooren, Bas, Fuller, Joel T., Buckley, Jonathan D., Miller, Jayme R., Sewell, Kerry, Rao, Guillaume, Barton, Christian, Bishop, Chris, Willy, Richard W., 2020. Is Motorized Treadmill Running Biomechanically Comparable to Overground Running? A Systematic Review and Meta-Analysis of Cross-Over Studies. *Sports Med.* 50 (4), 785–813.